

Article

Improving the Wear Resistance of Moulds for the Injection of Glass Fibre–Reinforced Plastics Using PVD Coatings: A Comparative Study

Francisco Silva ^{1,*}, Rui Martinho ¹, Maria Andrade ¹, António Baptista ² and Ricardo Alexandre ³

¹ ISEP—School of Engineering, Polytechnic of Porto, 4200-072 Porto, Portugal; rpm@isep.ipp.pt (R.M.); mfga@isep.ipp.pt (M.A.)

² INEGI—Instituto de Ciéncia e Inovação em Engenharia Mecânica e Engenharia Industrial, 4200-465 Porto, Portugal; amb@fe.up.pt

³ TEAndM—Tecnologia, Engenharia e Materiais; 3045-508 Taveiro, Portugal; ricardo@teandm.pt

* Correspondence: fgs@isep.ipp.pt; Tel.: +351-228-340-500

Academic Editor: Alessandro Lavacchi

Received: 31 December 2016; Accepted: 9 February 2017; Published: 16 February 2017

Abstract: It is well known that injection of glass fibre–reinforced plastics (GFRP) causes abrasive wear in moulds’ cavities and runners. Physical vapour deposition (PVD) coatings are intensively used to improve the wear resistance of different tools, also being one of the most promising ways to increase the moulds’ lifespan, mainly when used with plastics strongly reinforced with glass fibres. This work compares four different thin, hard coatings obtained using the PVD magnetron sputtering process: TiAlN, TiAlSiN, CrN/TiAlCrSiN and CrN/CrCN/DLC. The first two are monolayer coatings while the last ones are nanostructured and consist of multilayer systems. In order to carry out the corresponding tribological characterization, two different approaches were selected: A laboratorial method, using micro-abrasion wear tests based on a ball-cratering configuration, and an industrial mode, analysing the wear resistance of the coated samples when inserted in a plastic injection mould. As expected, the wear phenomena are not equivalent and the results between micro-abrasion and industrial tests are not similar due to the different means used to promote the abrasion. The best wear resistance performance in the laboratorial wear tests was attained by the TiAlN monolayer coating while the best performance in the industrial wear tests was obtained by the CrN/TiAlCrSiN nanostructured multilayer coating.

Keywords: PVD coating; sputtering; wear behaviour; TiAlN; TiAlSiN; diamond-like carbon (DLC); injection moulds; abrasion; glass-fibre reinforced plastics (GFRP)

1. Introduction

Injection moulding is probably the most widely used plastics manufacturing technology. Nowadays, increasing requirements demanded by designers have driven the use of short glass fibers as reinforcements in many parts, namely for the automotive industry. Abrasion is a typical phenomenon in the plastic injection moulding process and it becomes even more important when plastics are reinforced with glass fibres [1–5]. Otherwise, maintenance operations related to moulds represent the costs and inactivity periods of the mould which affect the competitiveness of the process and are strongly connected to the concept of the life cycle cost [6].

New developments in the polymer industry led to the use of new polymer formulations and blends that are more and more aggressive to steel mould cavities due to gases generated into the mould, causing serious corrosion problems, which bring new challenges to the coatings research and industry [7]. This problem is magnified by the temperature effect [8], and it is even more important

when we are talking about lighting reflector systems and other automotive parts where transparency and/or surface quality are critical requirements for the customer and no scratches or other scars are allowed [7]. The Fresnel lens, manufactured by injection moulding, also requires a high quality level, preventing the occurrence of any kind of superficial defects in the mould cavities [9]. In these cases, usually no reinforcements are applied, and the corrosion and the high pressures exerted into the mould are the main problems to overcome.

However, despite some other important issues related to mould cavity degradation, such as adhesion and fatigue, abrasion plays an important role, severely affecting the surface quality of the mould and, subsequently, the quality and brightness of the injected part's surface. Indeed, the natural motion of the fibre tips during the injection flow induces small scratches both in the screw and barrels of the injection machine as well as in the mould cavity, leading to bright degradation of the mould cavity surface. Tribological problems associated with the plastics moulding process can often be solved by an appropriate surface modification. Several techniques can be efficient to increase the wear behaviour of the mould cavity surface or other mechanical tools, such as ion implantation, physical vapour deposition (PVD), chemical vapour deposition (CVD), and standard diffusion processes, namely plasma nitriding [10–13].

Some authors even developed test models in order to simulate the tribological mechanisms involved inside the injection machine barrel, but without complete success, because only some of the main wear mechanisms were effectively tested [14]. However, there are other subjects that deserve our attention, namely the heat insulation and/or heat transfer phenomena that cannot be neglected with the coating application, constituting a new concern in the coating selection process [15]. Effectively, the coating must help to improve the wear resistance but it must also help to maintain or even decrease the injection cycle time, leading to a productivity improvement by keeping or improving the part cooling process after injection.

In order to overcome these problems, some authors have investigated a diversified number of surface treatments and tribological coatings [1–3,5,15–20]. In fact, recent developments in coatings technology allow a multifaceted approach to each problem, using mono- or multilayered coatings, single composition or graded layers, conventional or nanostructured films. More recently, some authors have tested selected films by submitting them to real injection conditions [1–3,21], obtaining results that allow us to think that coatings should be applied to moulds in a competitive way. The wear improvement of some steel mould inserts was also tested using a polycrystalline diamond [22] provided with an interlayer in order to avoid the diffusion of C into the Fe (substrate).

In this work, two dissimilar approaches were conducted using different coating concepts: two monolayer films (TiAlN and TiAlSiN) and two multilayer nanostructured coatings (CrN/TiAlCrSiN and CrN/CrCN/DLC). The main goal of this work was to characterise and compare the wear behaviour of these coatings under real conditions of plastic injection moulding, using glass fibre-reinforced polypropylene. This work also intended to find a competitive way to increase the life cycle of the moulds, minimizing maintenance operations and costs.

2. Materials and Methods

2.1. Substrates Material and Preparation

Plastic injection moulds manufacturers typically use AISI P20 tool steel (Bohler Uddeholm, Vienna, Austria) as main material for mould cavities, which is usually supplied in the hardened state. Thus, this material was used as substrate for this work. AISI P20 steel was subject to mass spectroscopy analysis and the chemical composition (wt %) obtained was the following one: 0.35% C, 0.29% Si, 1.95% Cr, 1.39% Mn, 0.19% Mo, 1.00% Ni and 0.01% S. The hardness of the steel was assessed using a universal hardness tester EMCO (model M4U, EMCO-TEST Prüfmaschinen GmbH, Kellau, Kuchl, Austria) carrying out five tests and taking the average value of 380 HBW 2.5/187.5/5. In order to carry out the wear tests, two different kinds of samples were used: laboratorial samples with a quadrangular

shape of 25 mm × 25 mm and 2 mm thickness, and industrial samples with a specific shape allowing its insertion on proper cavities machined in the mould, allowing the contact of the samples with the plastic flow during each injection cycle. The cavities dug into the mould have a slight conical shape, allowing a better adjustment of the samples in the cavity. The shape of the industrial samples can be observed in Figure 1. These samples were placed in the plastic feed channel of the mould, letting its surface coincident with the remaining surface of the feed channel. Surface of both kind of samples was milled in a Computer Numeric Control machining centre and further ground until an average surface roughness of 0.06 μm has been retrieved, which is enough to observe wear phenomena and is similar to surface roughness usually used in this kind of injection tools.

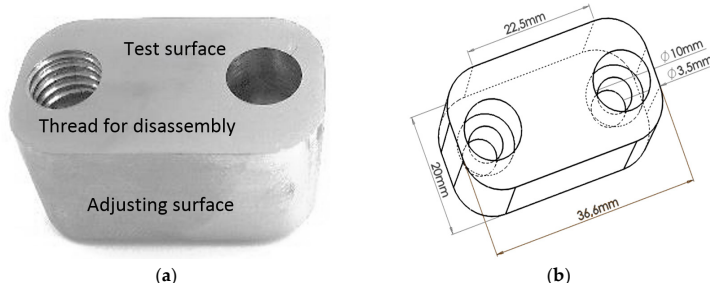


Figure 1. Industrial sample shape and corresponding dimensions: (a) view of the inserts used in the moulds and (b) corresponding dimensions.

2.2. Coatings Deposition

Coatings were produced using a CemeCon CC800/9 PVD unbalanced magnetron sputtering reactor (CemeCon, A.G., Wurselen, Germany). The following deposition parameters were similar for every coatings here referred: Gas pressure 500 mPa, Temperature 500 °C, Target power density 16 A·cm⁻², Bias in the range of −120 V to −50 V, and deposition time 4 h. However, in order to produce each coating, different targets and gases were used, as pointed in Table 1, which summarises these conditions.

Table 1. Targets and gases used in the coatings deposition process.

Coating	Targets	Gases
TiAlN	TiAl ($\times 4$)	N
TiAlSiN	TiAlSi ($\times 4$)	N
CrN/TiAlCrSiN	TiAlSi ($\times 2$) + Cr ($\times 2$)	N
CrN/CrCN/DLC	Cr ($\times 2$) + Graphite ($\times 2$)	Ar ⁺ + N + C ₂ H ₂

In order to ensure the correct exposure of the samples to the targets and the best homogeneity of the films, sample's holder was animated with a circular motion of 1 rotation per minute.

In the particular case of the CrN/CrCN/DLC multi-layered coating, the CrN bottom and intermediate layers were generated from two Cr targets using N and Ar⁺ feed gas, when for the last one C₂H₂ was added to N and Ar⁺. For the top layer, the Cr targets were hidden behind the shutters and two graphite targets were exposed.

2.3. Coatings Characterization

After deposition, both film thickness and morphology were assessed by SEM (scanning electron microscopy, FEI, Hillsboro, OR, USA) using a FEI Quanta 400FEG scanning electron microscope provided with an EDAX Genesis X-ray spectroscope (EDS—energy dispersive spectroscopy, EDAX, Mahwah, NJ, USA). For the thickness measurement, a metallographic preparation was done; samples were partially cut in the reverse side of the coating and then they are submerged in liquid nitrogen

during 20 min in order to promote a brittle behavior. At that time, samples were taken and mechanically broken, minimizing by this way plastic deformations close to the cutting edge. Then, they were embedded in resin with cross section turned to the working face. Further, the assembled set was ground with F1200 sandpaper until main grooves disappear and then, it was polished with diamond grit solutions of 3 and 1 μm during 10 min each one. Surface morphology and roughness were also evaluated by Atomic Force Microscopy (AFM) (VEECO Instruments, Ltd., Woodbury, NY, USA) using a VEECO Multimode atomic force microscope system (7 nm tip radius) provided with the NanoScope 6.13 software (version 6.13, Bruker, New York, NY, USA). In these analyses, two different areas were considered: 10 $\mu\text{m} \times 10 \mu\text{m}$ and 50 $\mu\text{m} \times 50 \mu\text{m}$, comparing the results. A CAMECA Electron Probe Micro-Analysis (EPMA) system (SX-50 model, CAMECA Instruments, Inc., Madison, WI, USA) was also used equipped with wavelength dispersive spectroscopy (WDS) system (version 2.0, CAMECA Instruments, Inc., Madison, WI, USA), allowing confirm the coatings chemical composition. Micro-hardness was also quantified using Fischerscope[®] H100 equipment (Fischerscope, Windsor, CT, USA), provided with Vickers indenter. A normal load of 50 mN was selected keeping it constant during 30 s, avoiding by this way creep phenomena. This equipment produces a values chart that allows obtaining “load–depth” curves, which let to compute hardness and Young’s modulus values.

2.4. Adhesion Analysis

The adhesion between each coating and substrate was assessed by scratch test and Rockwell indentation. Scratch tests were carried out using a CSM REVETEST equipment (CSEM, Neuchatel, Switzerland) following the procedures recommended by the BS EN 1071-3 (2005) standard [23]. The normal load was increasing from 0 to 80 N using a growing up rate of 100 $\text{N}\cdot\text{min}^{-1}$ and the indenter sliding speed used was 10 $\text{mm}\cdot\text{min}^{-1}$. Regarding the surface texture effect due to grinding process, two orthogonal measurements were considered allowing to understand the texture effect on the adhesion failure mechanisms. In each orthogonal direction three tests were made in order to maximise the results accuracy. Then, grooves were carefully observed by optical microscopy, correlating the distance of the groove and film detachment phenomena detected on the scratch with the applied load in each point. The grooves observation lets identifying when cohesive and adhesive failures occur, allowing to determine the corresponding load. Another technique was also used permitting to confirm qualitative results. Following the VDI 3198:1991 standard [24], Rockwell indentations were done at 294 N (30 kgf) and 980 N (100 kgf) normal loads, using an EMCO M4U 025 Universal Hardness Tester (EMCO-TEST Prüfmaschinen GmbH, Kellau, Kuchl, Austria). Indentation borders were observed in order to identify the presence of cracks and its pattern.

2.5. Micro-Abrasion Tests

In order to evaluate the wear behaviour of the three coatings and obtain comparable results with other types of coatings, micro-abrasion test configuration is an accurate option, being perfectly suitable for thin films wear characterization. Thus, a PLINT TE 66 tribometer (Figure 2) using ball-cratering configuration was used. In this test, a ball of AISI 52100 steel with 25 mm diameter was used as counter body. This ball, initially in polished state, was etched using a 10% NITAL solution during 20 s, increasing its surface roughness and allowing better abrasive particles motion. These tests use abrasive slurry composed by 35.4 g of SiC F1200 powder (following FEPA 42-2:2006 standard [25]), with average particle size of 4.3 μm , standard deviation 1.4 μm , homogeneously distributed in 100 mL distilled water. This slurry is continuously stirred by a magnetic issue into a glass container, during the wear tests. The sample surface in test is pressed against the ball by a vertical bar sustained by a pivot system, rotating on it. The ball rotation speed was 80 rpm, corresponding to 0.105 $\text{m}\cdot\text{s}^{-1}$ and a normal load of 0.25 N was applied in all tests. Three different test lengths were agreed: 200, 500 and 700 cycles, corresponding to sliding distances of 15.71, 39.27 and 54.98 m, respectively. Attending each test conditions set, five different tests were carried out trying to increase the accuracy of the results. After the tests, all wear scars were observed by optical microscopy, using an OLYMPUS BX51M

microscope provided with 12.5 megapixel OLYMPUS digital camera and AnalySIS DOCU image software (version 5.0, Olympus, Tokyo, Japan). Some results were later explored by SEM, using the above-mentioned equipment.

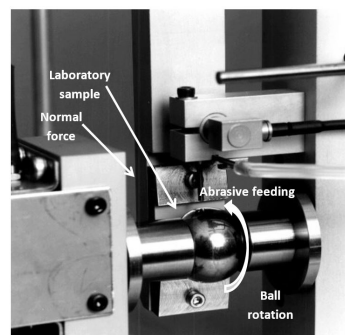


Figure 2. PLINT TE66 equipment (Phoenix Technology, London, UK) based on ball-cratering wear test configuration.

2.6. Industrial Wear Tests

As previously referred, the main objective of this work is to study the wear resistance of the coatings when applied in injection mould cavities used to produce glass fibre-reinforced plastic parts for automotive industry. Thus, an industrial mould often used for the production of radiator plastic fans was selected and three cavities symmetrically distributed and crossing the runners were machined into the mould allowing that samples surface fits well on the cavity due to the progressive section of the sample and cavity and allow that the sample exposed face is in the same plane of the mould surface in this area. The cavities were located centred on each plastic runner as depicted in Figure 3. During the injection cycle, glass fibre-reinforced plastic flows by the main feed channel (sprue) at the centre, being then split in three different ways. Arrows included in this figure intend to show the three directions of the plastic flow towards the secondary plastic feed channels (runners). These arrows were drawn over the sample cavities specially produced on the mould. Inserts were located in a turbulent area, in order to maximise the abrasive effect of the glass fibres, due to a previous quick flow direction shift. The composite used in the process is polypropylene reinforced with 30 wt % glass fibres and 9×10^4 injection cycles were performed allowing study the wear behaviour of the coating. It is well-known that, in these conditions, uncoated AISI P20 tool steel presents eye-visible severe wear scars. In these conditions, mould needs a complicate and expensive maintenance process, involving production breaks, accurate production plans and smart stock management or delivery delays. For this purpose, a KRAUSS MAFFEI injection machine (Krauss-Maffei Wegmann GmbH & Co. KG, Munich, Germany) was used presenting 5000 kN clamp force and inner initial pressure of 140 bar on the mould. The injection speed used was $50 \text{ m} \cdot \text{s}^{-1}$ and injection temperature was about 250°C .

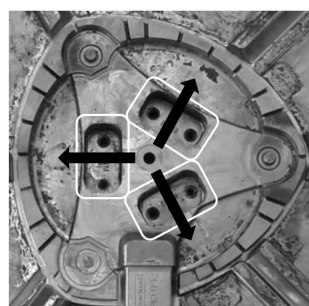


Figure 3. Industrial wear tests setup, showing the cavities location in the mould (white boxes) and the plastic flow (black arrows).

3. Results and Discussion

The chemical composition of the films was evaluated using electron-probe microanalysis. The results can be seen in Table 2, showing that the compositions are in line with the targets and gases used in the deposition process and fulfil the initial expectations. The coatings' thickness was assessed by SEM, leading to the values listed in Table 3, in the range of 3.5 to 4.5 μm , as desired, having been controlled by both the deposition rate and time. The morphology of the coatings was analysed by SEM as well, denoting that the films tend to follow the substrate topography, keeping the thickness approximately constant along the surface. The coatings' surface was relatively smooth, as shown in Figure 4, as expected when the films are produced using the magnetron sputtering technique. The nanostructured coating shown in Figure 4d corresponded to different CrCN phases, one of them more carbon-rich than the other, which was obtained providing C_2H_2 periodically and controlled over time. However, the TiAlSiN film presented some aggregates at the surface, which can originate from tribological problems, both through the generation of preferred sites for crack nucleation and problems related to the release of these large particles in contact the counter-face. The roughness was evaluated by profilometry and yields to confirm that Ra values were in the range of 0.033 μm to 0.061 μm for all coatings. The R_a values obtained by the AFM evaluation were slightly different, varying in the range of 0.028 μm to 0.053 μm , this difference being mainly attributed to the lower area of analysis. The values obtained are in line with the requirements usually defined for inner mould surfaces for the plastic injection moulding of non-visible automotive parts, such as the case studied in this work. The micro-hardness was measured using different techniques due to the low thickness of the CrN/CrCN/DLC final layers, revealing that the hardest coating was the CrN/TiAlCrSiN coating and the softest was the CrN/CrCN/DLC coating. Taking into account the curves' load/depth of displacement of the indenter generated by the micro-hardness equipment, Young's modulus was also assessed, allowing us to compute the reduced Young's modulus, the values of which are shown in Table 3, which allowed us to compute the values of the H^3/E_r^2 ratio, a good indicator for the coatings' resistance to plastic deformation. In this case, the best and worst plastic deformation resistance was presented by CrN/TiAlCrSiN and CrN/CrCN/DLC coatings, respectively. Believing just in the hardness values obtained, the CrN/TiAlCrSiN coating would present the best wear resistance due to it having highest value in the range of coatings tested in this work.

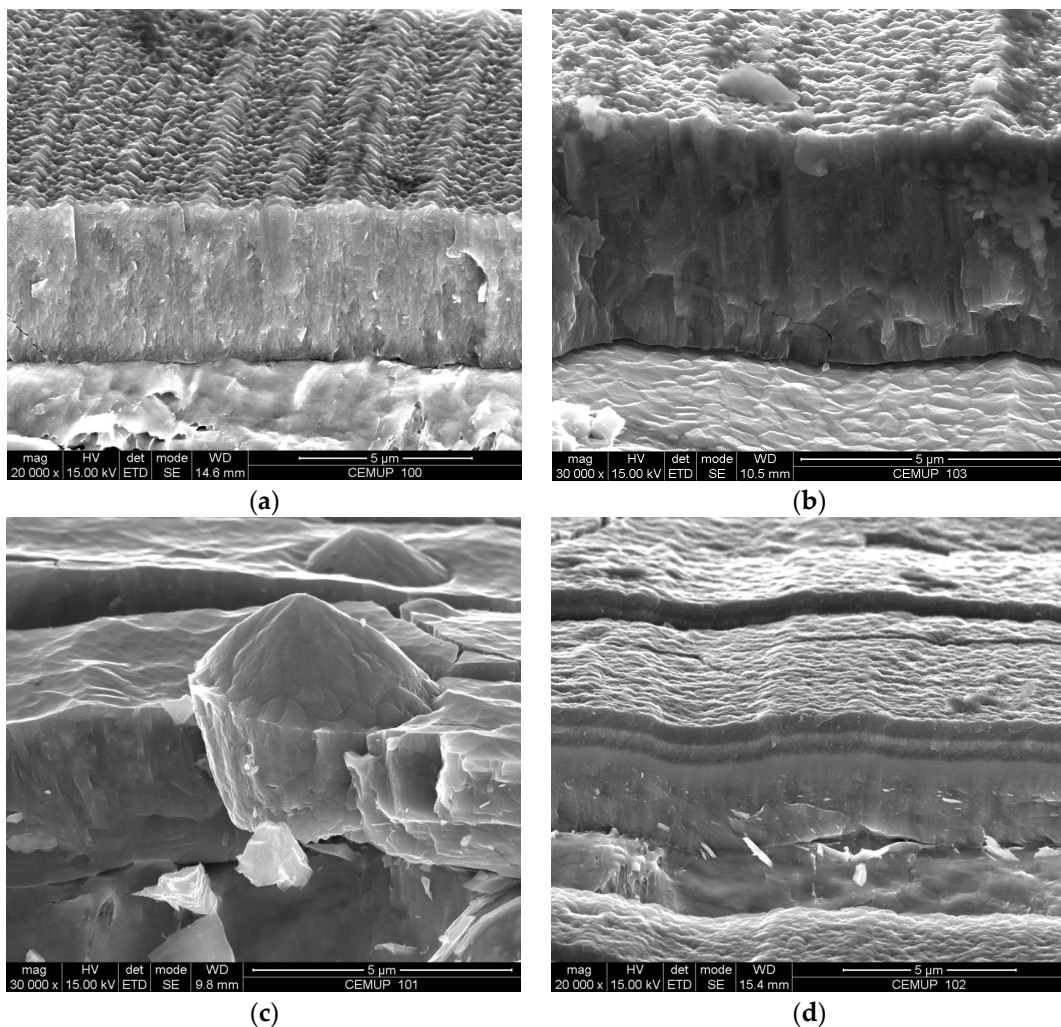
Adhesion tests were carried out using two different techniques: scratch tests and indentation tests, as described in the Experimental Section. The scratches produced during the tests were carefully analysed by optical microscopy and allowed us to observe some typical phenomena usually occurring in these tests, namely conformal cracking (TiAlSiN) plus lateral chipping (TiAlN), coating delamination in the scratch channel and lateral cracking (CrN/TiAlCrSiN). In general, the critical loads that caused the coatings' failure in these tests were below the expectations. These values varied between 20 and 25 N, considering the two orthogonal directions selected. Films with similar compositions usually present critical loads for adhesion or cohesion failure at about 70 or even 75 N. Thus, the indentation technique was also used in order to cross the results and to guarantee that the coatings' adhesion was enough to continue to the wear tests. Except the CrN/CrCN/DLC coating, all coatings were subject to indentation tests using 30 and 100 kgf as described in the Experimental Section and subsequently observed by optical microscopy, allowing us to observe that indentation borders presented mainly a cracking pattern of small radial cracks in all the films observed. Despite some reports that CrN-based coatings present delamination in the borders of the indentation [26], no delaminations were observed in the samples used in this work. Thus, all the films were considered suitable for wear tests.

Table 2. Chemical characterization of the coatings (performed by EPMA).

Coating	N (at.%)	O (at.%)	Al (at.%)	Si (at.%)	Ti (at.%)	Cr (at.%)
TiAlN	49.77 ± 1.09	1.17 ± 0.17	26.91 ± 0.67	—	22.15 ± 0.47	—
TiAlSiN	46.24 ± 0.49	1.33 ± 0.17	10.56 ± 0.14	4.56 ± 0.04	37.31 ± 0.48	—
CrN/TiAlCrSiN	44.92 ± 1.91	—	2.55 ± 0.19	1.26 ± 0.08	1.290 ± 0.11	49.97 ± 1.60
CrN/CrCN/DLC				Not evaluated		

Table 3. General characterization of the coatings (performed by profilometry and AFM).

Coating	Thickness (μm)	Roughness (R_a , μm)	Roughness (R_t , μm)
Uncoated	—	0.060 ± 0.005/0.051 ± 0.002	0.365 ± 0.018/0.312 ± 0.009
TiAlN	3.5 ± 0.2	0.058 ± 0.006/0.049 ± 0.003	0.517 ± 0.029/0.488 ± 0.021
TiAlSiN	4.5 ± 0.3	0.061 ± 0.004/0.053 ± 0.003	0.635 ± 0.021/0.598 ± 0.023
CrN/TiAlCrSiN	4.3 ± 0.4	0.033 ± 0.003/0.028 ± 0.001	0.414 ± 0.011/0.375 ± 0.013
CrN/CrCN/DLC	3.6 ± 0.2	0.054 ± 0.005/0.045 ± 0.002	0.385 ± 0.010/0.351 ± 0.008

**Figure 4.** Morphological characterization of the following coatings: (a) TiAlN; (b) TiAlSiN; (c) CrN/TiAlCrSiN and (d) CrN/CrCN/DLC assessed by SEM.

The micro-abrasion tests were carried out following the conditions already mentioned in the Experimental Section. Due to the low thickness of the films, after some ball revolutions in the micro-abrasion tests, the coating was consumed by abrasion and just the film border prevented greater wear [27]. Thus, in these cases, it was necessary to measure the inner and outer diameter of the

crater, which corresponded to the substrate and coating-resistant area. In order to analyse the coatings' behaviour, just the removed material corresponding to the coating was considered for calculations (c —coating). The results showed that the wear coefficient (k_c) was the smallest for the TiAlN coating while it was the greatest for the CrN/TiAlCrSiN coating, corresponding to the better wear resistance (k^{-1}) of the TiAlN coating, which also presented a relatively low reduced Young's modulus. The results summary of these tests can be seen in Table 4. Figure 5 depicts the usual shape of each crater with the typical border corresponding to the film's resistant thickness, whereas the inner area corresponds to the substrate that was in contact with the ball and the abrasive slurry after coating perforation. Figure 5b shows the typical way out border of the slurry, displaying how the abrasive particles scratched the coating into the crater, reducing this effect as the ball left the contact area of the sample. As shown in Table 4, regarding just the micro-abrasion tests, the best wear behaviour was shown by the CrN/TiAlCrSiN coating, allowing a useful lifespan 65.5 times greater than the uncoated substrate. However, these tests should be considered comparative, using the wear resistance already obtained and computed in similar conditions when testing other coatings. The wear phenomena expected in the plastic injection moulding process are quite different, just because the difference in the hardness between materials and the density of abrasive particles present in the contact are also quite different.

Table 4. Hardness and micro-abrasion wear resistance of the coatings used in this work.

Coating	Thickness (μm)	Hardness (Gpa)	E (GPa)	E_r (Gpa)	H^3/E^2 (Gpa)	k_c ($\text{mm}^3/\text{N}\cdot\text{m}$)	k^{-1} ($\text{N}\cdot\text{m}/\text{mm}^3$)
TiAlN	3.5 ± 0.2	22.7 ± 1.2	392	304	0.076	6.51E-5	15.37
TiAlSiN	4.5 ± 0.3	21.8 ± 1.7	491	282	0.043	24.6E-5	4.068
CrN/TiAlCrSiN	4.3 ± 0.4	30.9 ± 2.1	422	325	0.166	37.3E-5	2.683
CrN/CrCN/DLC	3.6 ± 0.2	19.2 ± 1.1	340	288	0.061	31.8E-5	3.141

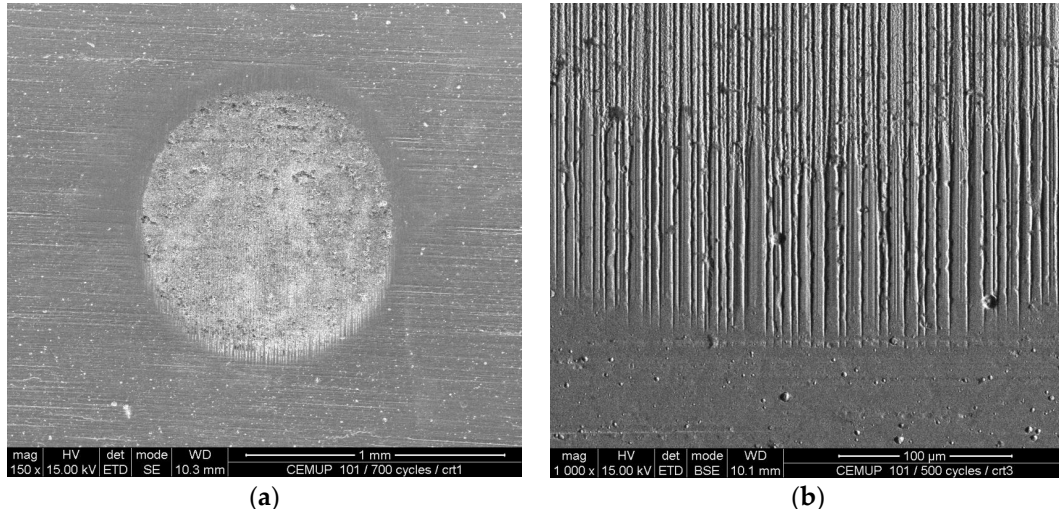


Figure 5. (a) Crater pattern and (b) border detail corresponding to wear test of the CrN/TiAlCrSiN coating after 700 wear cycles in the TE66 PLINT Tribometer under the test conditions mentioned above.

Assuming that industrial tests could lead to significantly different results, the industrial tests were performed by inserting three different samples into cavities previously machined in the mould and adjusting them in order to keep their surface on the same plane of the remaining inner surface of the mould. Thus, the reinforced plastic could flow through the feed channels, tangentially abrading the mould and sample surface during its motion along the feed channels, with some turbulence caused by the directional flow shift of the reinforced plastic close to the sample's position. Each sample was provided with a different coating, allowing us to test three different coatings in each setup. The injection conditions and reinforced plastic properties had already been previously announced.

After 9×10^4 injection cycles, the lowest volume of the coating removed by abrasion and adhesion was achieved by the hardest multilayer coating, CrN/TiAlCrSiN. The results in this test were obtained by analysing the material removed from the surface due to the glass fibres' abrasion during the injection cycle runs, as can be seen in Figure 6. The surface of the coatings was analysed by SEM and wear scars or detachments were identified by computed with homemade software (PAQI) which allows us to determine the percentage of the coating area removed. Complementary EDS tests were also conducted in order to verify the absence of coating in those areas.

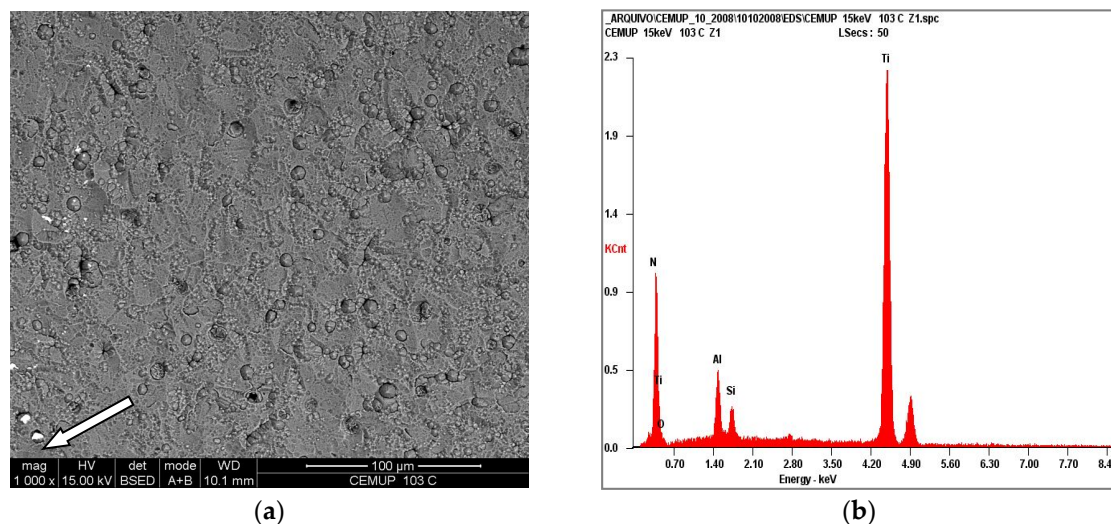


Figure 6. (a) Coating surface view after 90,000 injection cycles, denoting some punctual wear close to the left border of the image and (b) corresponding EDS analysis of the points indicated by the white arrow.

The thickness of the coatings was already analysed by profilometry, based on the surface of the samples not exposed to the plastic flow. The results can be seen in Table 5.

Table 5. Industrial wear test results summary.

Coating	Hardness (GPa)	Removed Height (μm)	Removed Coating Area (%)	Life vs. Steel
TiAlN	22.7 ± 1.2	0.035 ± 0.003	0.125 ± 0.005	$30.8 \times$
TiAlSiN	21.8 ± 1.7	0.049 ± 0.006	0.134 ± 0.003	$25.0 \times$
CrN/TiAlCrSiN	30.9 ± 2.1	0.014 ± 0.003	0.013 ± 0.001	$65.5 \times$
CrN/CrCN/DLC	19.2 ± 1.1	0.017 ± 0.004	0.032 ± 0.002	$58.2 \times$

Regarding these last results, the hardness seems to play an important role in the wear behavior of the multilayered coating when submitted to the injection of reinforced polypropylene. On the other hand, TiAlN presented the best wear behavior when submitted to micro-abrasion tests, even presenting a lower hardness than the CrN/TiAlCrSiN coating and also a relatively low H3/E2 ratio, showing low resistance to plastic deformation. Thus, this work allowed us to observe that micro-abrasion tests cannot be used to predict the coating lifespan when applied to mould cavities for the reinforced plastic injection moulding process.

4. Conclusions

Four different coatings were deposited, characterised and tested using two different methods in order to verify their ability to be used in mould cavities for the reinforced plastic injection moulding process. After all analyses and tests, some conclusions can be drawn, as follows:

- The morphology of the coatings is adequate for use in mould cavities of the reinforced plastic injection moulding process, allowing roughnesses (R_a) in the range of 0.033 and 0.061 μm (results obtained by profilometry).
- The coatings' adhesion, measured by scratch-test method, was low, allowing us to observe the failure mechanisms of the films in the scratches. However, indentation tests revealed that no indentation border detachments were observed, showing that the coatings' adhesion was enough to ensure the best wear resistance of the films.
- Micro-abrasion ball-cratering tests allowed us to determine that, under these wear conditions, the most wear-resistant coating in the range considered in this work was the TiAlN monolayered coating. However, as previously mentioned, these test conditions cannot be compared with the wear mechanisms usually performed in the reinforced plastic injection process due to different means used to promote the abrasion, i.e., SiC abrasive particle in the case of the lab tests and glass fibres in the case of industrial tests. The different hardness presented by these means endorses different responses of the coated surfaces.
- Industrial tests revealed that the best coating under the plastic injection conditions was the CrN/TiAlCrSiN coating, allowing a considerable lifespan benefit that was 65.5 times greater than that of the uncoated substrate.

Thus, considering these results, the industry can adopt the CrN/TiAlCrSiN coating as the best choice in terms of the wear caused by the glass fibre tips due to their random motion during the injection process.

Acknowledgments: The authors gratefully acknowledge the financial support of INEGI—Instituto de Ciência e Inovação em Engenharia Mecânica e Engenharia Industrial as well as the permission to use their facilities. The strong cooperation of the TEandM—Tecnologia, Engenharia e Materiais, S.A. and Plastaze—Plásticos de Azeméis, S.A. (SIMOLDES Group) companies is also deeply acknowledged.

Author Contributions: Francisco Silva conceived and designed the experiments and wrote the paper; Rui Martinho performed the experiments, collected the data and made the critical analyses; Maria de Fátima Andrade prepared all samples; António Baptista analysed the data, provided critical analyses and supervised all works; Ricardo Alexandre provided the coatings and helped in critical analyses.

Conflicts of Interest: The authors declare no conflict of interest.

References

1. Martinho, R.P.; Silva, F.J.G.; Alexandre, R.J.D.; Baptista, A.P.M. TiB₂ Nanostructured Coating for GFRP Injection Moulds. *J. Nanosci. Nanotechnol.* **2011**, *11*, 5374–5382. [[CrossRef](#)]
2. Silva, F.J.G.; Martinho, R.P.; Alexandre, R.J.D.; Baptista, A.P.M. Wear Resistance of TiAlSiN Thin Coatings. *J. Nanosci. Nanotechnol.* **2012**, *12*, 9094–9101. [[CrossRef](#)] [[PubMed](#)]
3. Silva, F.J.G.; Casais, R.C.B.; Martinho, R.P.; Baptista, A.P.M. Mechanical and Tribological Characterization of TiB₂ Thin Films. *J. Nanosci. Nanotechnol.* **2012**, *12*, 9187–9194. [[CrossRef](#)] [[PubMed](#)]
4. Silva, F.J.G.; Martinho, R.P.; Baptista, A.P.M. Characterization of laboratory and industrial CrN/CrCN/diamond-like carbon coatings. *Thin Solid Films* **2014**, *550*, 278–284. [[CrossRef](#)]
5. Bobzin, K.; Brögelmann, T.; Grundmeier, G.; de los Arcos, T.; Wiesing, M.; Kruppe, N.C. (Cr,Al)N/(Cr,Al)ON Oxy-nitride Coatings deposited by Hybrid dcMS/HPPMS for Plastics Processing Applications. *Surf. Coat. Technol.* **2016**, *308*, 394–403. [[CrossRef](#)]
6. Folgado, R.; Peças, P.; Henriques, E. Life cycle cost for technology selection: A Case study in the manufacturing of injection moulds. *Int. J. Prod. Econ.* **2010**, *128*, 368–378. [[CrossRef](#)]
7. Mitterer, C.; Holler, F.; Reitberger, D.; Badisch, E.; Stoiber, M.; Lugmair, C.; Nobauer, R.; Muller, T.; Kullmer, R. Industrial applications of PACVD hard coatings. *Surf. Coat. Technol.* **2003**, *163*, 716–722. [[CrossRef](#)]
8. Boey, P.; Ho, W.; Bull, S.J. The effect of temperature on the abrasive wear of coatings and hybrid surface treatments for injection-moulding machines. *Wear* **2005**, *258*, 149–156. [[CrossRef](#)]
9. Tosello, G.; Hansen, H.N.; Gasparin, S.; Albajez, J.A.; Esmoris, J.I. Surface wear of TiN coated nickel tool during the injection moulding of polymer micro Fresnel lenses. *CIRP Ann. Manuf. Technol.* **2012**, *61*, 535–538. [[CrossRef](#)]

10. Fox-Rabinovich, G.S.; Yamamoto, H.; Kovalev, A.I.; Veldhuis, S.C.; Ning, L.; Shuster, L.S.; Elfizy, A. Wear behavior of adaptive nano-multilayered TiAlCrN/NbN coatings under dry high performance machining conditions. *Surf. Coat. Technol.* **2008**, *202*, 2015–2022. [[CrossRef](#)]
11. Bouzakis, K.-D.; Pappa, M.; Skordaris, G.; Bouzakis, E.; Gerardis, S. Correlation between PVD coating strength properties and impact resistance at ambient and elevated temperatures. *Surf. Coat. Technol.* **2010**, *205*, 1481–1485. [[CrossRef](#)]
12. Dosbaeva, G.K.; Veldhuis, S.C.; Yamamoto, K.; Wilkinson, D.S.; Beake, B.D.; Jenkins, N.; Elfizye, A.; Fox-Rabinovich, G.S. Oxide scales formation in nano-crystalline TiAlCrSiYN PVD coatings at elevated temperature. *Int. J. Refract. Met. Hard Mater.* **2010**, *28*, 133–141. [[CrossRef](#)]
13. Bouzakis, K.-D.; Klocke, F.; Skordaris, G.; Bouzakis, E.; Gerardis, S.; Katirtzoglou, G.; Makrimallakis, S. Influence of dry micro-blasting grain quality on wear behaviour of TiAlN coated tools. *Wear* **2011**, *271*, 783–791. [[CrossRef](#)]
14. Bull, S.J.; Zhou, Q. A simulation test for wear in injection moulding machines. *Wear* **2001**, *249*, 372–378. [[CrossRef](#)]
15. Chen, S.-C.; Chang, Y.; Chang, Y.-P.; Chen, Y.-C.; Tseng, C.-Y. Effect of cavity surface coating on mold temperature variation and the quality of injection molded parts. *Int. Commun. Heat Mass Transfer* **2009**, *36*, 1030–1035. [[CrossRef](#)]
16. Bull, S.J.; Davidson, R.I.; Fisher, E.H.; McCabe, A.R.; Jones, A.M. A simulation test for the selection of coatings and surface treatments for plastics injection molding machines. *Surf. Coat. Technol.* **2000**, *130*, 257–265. [[CrossRef](#)]
17. Van Stappen, M.; Vandierendonck, K.; Mol, C.; Beeckman, E.; De Clercq, E. Practice vs. laboratory tests for plastic injection moulding. *Surf. Coat. Technol.* **2001**, *142–144*, 143–145. [[CrossRef](#)]
18. Cunha, L.; Andritschky, M.; Pischedow, K.; Wang, Z.; Zarychta, A.; Miranda, A.S.; Cunha, A.M. Performance of chromium nitride and titanium nitride coatings during plastic injection moulding. *Surf. Coat. Technol.* **2002**, *153*, 160–165. [[CrossRef](#)]
19. Santos, C.S.C.; Neto, V. Nanostructured coatings in micromoulding injection—A case study. *Mater. Today Proc.* **2015**, *1*, 414–422. [[CrossRef](#)]
20. Ozturk, O.; Onmus, O.; Williamson, D.L. Microstructural, mechanical, and corrosion characterization of nitrogen-implanted plastic injection mould steel. *Surf. Coat. Technol.* **2005**, *196*, 333–340. [[CrossRef](#)]
21. Stock, H.-R.; Diesselberg, M.; Zoch, H.-W. Investigation of magnetron sputtered titanium–nickel–nitride thin films for use as mould coatings. *Surf. Coat. Technol.* **2008**, *203*, 717–720. [[CrossRef](#)]
22. Neto, V.F.; Vaz, R.; Oliveira, M.S.A.; Grácio, J. CVD diamond-coated steel inserts for thermoplastic mould tools—Characterization and preliminary performance evaluation. *J. Mater. Process. Technol.* **2009**, *209*, 1085–1091. [[CrossRef](#)]
23. *BS EN 1071-3 Advanced Technical Ceramics, Methods of Test for Ceramic Coatings-Determination of Adhesion and Other Mechanical Failure Modes by a Scratch Test*; British Standards Institution: London, UK, 2005.
24. *VDI 3198-Beschichten von Werkzeugen der Kaltmassivumformung CVD- und PVD-Verfahren*; Verein Deutscher Ingenieure: Dusseldorf, Germany, 1991.
25. *FEPA Standard 42-2-Grains of Fused Aluminium Oxide, Silicon Carbide and Other Abrasive Materials for Bonded Abrasives and for General Industrial Applications Microgrits F230 to F2000*; Federation of European Producers of Abrasives: Darmstadt, Germany, 2006.
26. Vidakis, N.; Antoniadis, A.; Bilalis, N. The VDI 3198 indentation test valuation of a reliable qualitative control for layered compounds. *J. Mater. Process. Technol.* **2003**, *143*, 481–485. [[CrossRef](#)]
27. Kusano, Y.; Van, A.K.; Hutchings, I.M. Methods of data analysis for the micro-scale abrasion test on coated substrates. *Surf. Coat. Technol.* **2004**, *183*, 312–327. [[CrossRef](#)]

